Analytical investigation on bond behavior between concrete and FRP bars of near-surface mounted and embedded through-section strengthening methods

Nakares Kongmalai[1,*], Linh Van Hong Bui[2] and Pitcha Jongvivatsakul[3]

[1,3] Innovative Construction Materials Research Unit, Department of Civil Engineering, Faculty of Engineering, Chulalongkorn University, Bangkok, THAILAND

[2] Faculty of Civil Engineering, Industrial University of Ho Chi Minh City, Ho Chi Minh, VIETNAM

** Corresponding author; E-mail address: nakares44@gmail.com*

Abstract

The strengthening techniques are to enhance the performance of existing reinforced concrete (RC) structures. This research aims to investigate the bond behavior between fiber-reinforced polymer (FRP) bars and concrete interfaces of near-surface mounted (NSM) strengthening method and the embedded through-section (ETS) strengthening technique. Bond models for two strengthening methods are developed considering various crucial parameters. The effects of concrete compressive strength, embedment length, and modulus of elasticity of FRP bars on the bond responses between two retrofitting methods are analytically investigated to interpret the results through bond models.

Keywords: Bond behavior, Fiber-reinforced polymer, Near-surface mounted, Embedded through-section, Strengthening

1. Introduction

Nowadays, the huge challenge is to improve the performance of the existing reinforced concrete (RC) structures for extending their service life. Therefore, new materials are created to partially response the mentioned challenge. Presently, fiber-reinforced polymer (FRP) rods are one of feasible materials to enhance the structural efficiency instead of using conventional steel. Owing to the considerable properties of FRP materials, the repairing and strengthening using FRP composites are the reasonable ways to mitigate deterioration of RC structures.

Currently, there are two common methods for strengthening of the deteriorated RC structures. One is near-surface mounted (NSM) technique, in which the FRP was installed to the concrete surface with an adhesive [1-6]. Another technique is the embedded through-section (ETS) technique, which FRP rods with an adhesive were embedded into the predrilled holes through the section of members [7-9]. The strengthening configurations for these methods are demonstrated in **Fig. 1(a) and (b)**.

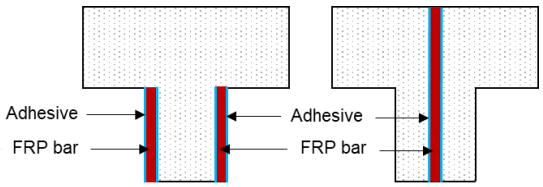

Fig. 1 The shear strengthening technique configurations: (a) NSM; (b) ETS

For both strengthening techniques, as revealed by Lorenzis et al. [1], Dai et al. [5] and Bui et al. [7], the interfacial response between FRP and concrete is an important factor that affect the performance of the structures; thus, it is necessary to consider carefully the bonding mechanism of FRP to concrete. Number of previous studies [1-9] indicated that the bond between concrete and FRP could be explained by the analysis of the bond stress—slip relationship through experiments and models. However, there is no clear research that discussed and assessed the efficiency of those strengthening techniques.

This study aims to investigate the bond performance of the ETS and NSM strengthening methods based the results of previous research. First, the available test data for ETS and NSM methods are used to propose the reliable bond models for each method. Then, the parametric study, which examines the effects of concrete compressive strength, Young's modulus of FRP, and embedment length, using the proposed interfacial bond model is carried out to evaluate the efficiency of the ETS and NSM techniques.

2. Development of bond model

2.1 Conceptual bond behavior

Fig. 2 shows the free-body diagrams of interface between FRP bars and concrete. The force components in **Fig. 2** can be written following equilibrium condition as Eq. (1).

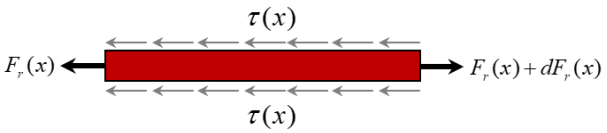

Fig. 2 The free-body diagrams between FRP bars and concrete [7]

$$dF_r(x) = A_r d\sigma_r(x) = p_r \tau(x) dx \quad (1)$$

where, $dF_r(x)$ is axial forces in the FRP bar at section dx, A_r is cross-sectional area of bars, $d\sigma_r(x)$ is tensile stress in the bar, p_r is the perimeter of the bar, and $\tau(x)$ is bond stress.

Afterwards, the uniaxial constitutive relationship for the linear elastic FRP bars is expressed by Eq. (2).

$$F_r(x) = E_r A_r \varepsilon_r(x) \quad (2)$$

where, $F_r(x)$ is the axial force in x direction, E_r is the modulus of elasticity of the bar, and $\varepsilon_r(x)$ is the axial stain along with x direction.

The slip function in terms of length x along the embedment length is defined with $s(x)$. The second order differential calculus of $s(x)$ is defined as Eq. (3). Eq. (3) is then substituted into Eq. (2) to be Eq. (4) as shown below.

$$\frac{d^2 s(x)}{dx^2} = \frac{d\varepsilon_r(x)}{dx} \quad (3)$$

$$\frac{dF_r(x)}{E_r A_r dx} = \frac{p_r \tau(x)}{E_r A_r} \quad (4)$$

Dai et al. [5] and Bui et al. [7] indicated that the exponential function shall be appropriate to derive the strain-slip relationship at loaded end of FRP as illustrated in Eq. (5).

$$\varepsilon = f(s) = A(1 - e^{-Bs}) \quad (5)$$

where, A and B are the experimental parameters. Therefore, the bond stress-slip relationship is derived by Eq. (3) and Eq. (4), which the strain is substituted by Eq. (5), as follows:

$$\tau = \frac{E_r A_r}{p_r} A^2 B e^{-Bs}(1 - e^{-Bs}) \quad (6)$$

The interfacial fracture energy (G_f) is defined as follows:

$$G_f = \int_0^\infty \tau ds \quad (7)$$

Eq. (6) is substituted into Eq. (7) so that G_f can be obtained as below.

$$G_f = \frac{A^2 E_r A_r}{2 p_r} \quad (8)$$

Moreover, the theoretical maximum pullout force (P_{max}) can be expressed as follows:

$$P_{max} = E_r A_r \varepsilon_{max} = E_r A_r \lim_{s \to \infty} A(1 - e^{-Bs}) = E_r A_r A \quad (9)$$

where, ε_{max} is the maximum strain of FRP bars corresponding to the maximum bond stress. Furthermore, the factor A in Eq. (8) is substituted into Eq. (9). Then, P_{max} can be rewritten in new form as shown in Eq. (10).

$$P_{max} = E_r A_r \sqrt{\frac{2 G_f p_r}{E_r A_r}} \quad (10)$$

Additionally, from Eq. (6) , the maximum slip (s_{max}) that corresponding to the maximum bond stress (τ_{max}), which can be defined by $d\tau / ds = 0$, are shown below.

$$s_{max} = \frac{\ln 2}{B} \quad (11)$$

$$\tau_{max} = \frac{B G_f}{2} \quad (12)$$

2.2 Approach for B and G_f formulations

In the bond model proposed by Bui et al. [5] and Dai et al. [7], the interfacial factors, which are the bond ductility (B) and the bond energy (G_f), can be derived from the test results using the above equations. Based on experimental data, the parameters B and G_f can be simplified as equations containing the terms of the concrete compressive strength (f_c'), stiffness of FRP bars ($E_r A_r / p_r$), embedded length (L_b), and properties of adhesive (G_a / t_a) through a regression procedure [5,7]. The property of adhesive can be expressed by Eq. (13).

$$\frac{G_a}{t_a} = \frac{E_{ad}}{2t_a(1+\nu_a)} \quad (13)$$

where, E_{ad} is the elastic modulus of adhesive, t_a is thickness of adhesive, and ν_a is the Poisson's ratio of adhesive.

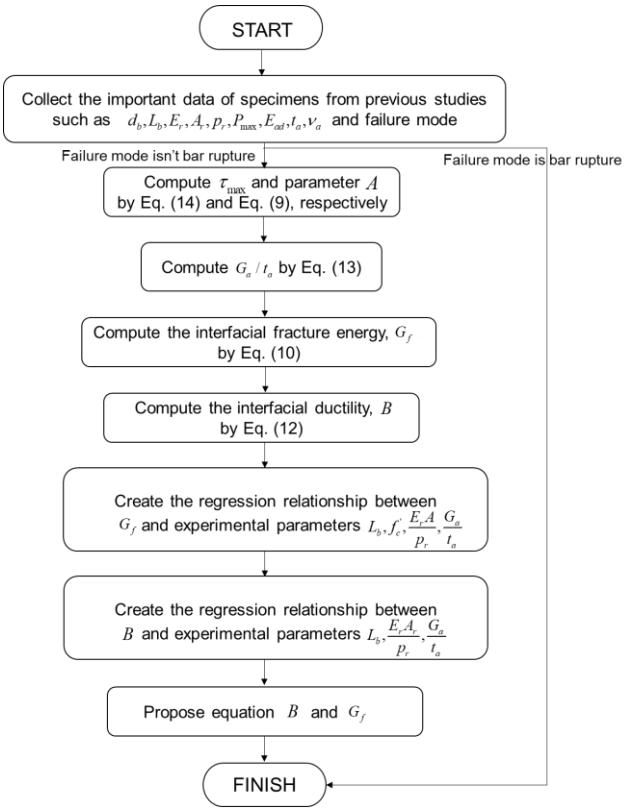

Fig. 3 The regression procedure considering all parameters

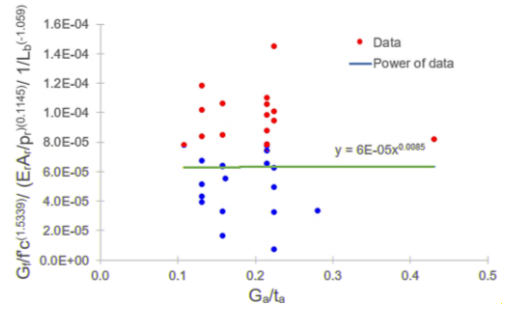

(a) Fracture energy (G_{f-ETS})

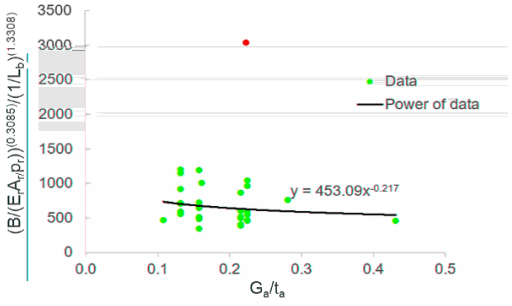

(b) Interfacial ductility (B_{ETS})

Fig. 4 The regression analysis of ETS strengthening technique

Additionally, the regression procedure considering all parameters is described in **Fig. 3**. The maximum bond stress can be calculated from Eq. (14). **Fig. 4** shows the example of the regression analysis of ETS method.

$$\tau_{max} = \frac{P_{max}}{\pi d_b L_b} \quad (14)$$

3. Proposed bond model

3.1 NSM strengthening method

3.1.1 Database

The total of 98 specimens tested by Lorenzis et al. [1], Soliman et al. [2], Hassan et al. [3], and Kalupahana [4] were used to formulate the bond model. The FRP bar properties used in formulation covered that the modulus of elasticities are in range of 31.17—174.71 GPa, the bar diameters are in range of 8.0—13.0 mm, and the embedment lengths are in range of 30.0—800.0 mm. The compressive strengths of concrete vary between 22—60 MPa. The properties of adhesive are in range of 0.345—1.493 GPa for elastic modulus and 1.0—7.95 mm for layer thickness.

3.1.2 Proposed formulations

Using the regression procedure analysis indicated in section 2, the bond factors for the NSM strengthening (G_{f-NSM} and B_{NSM}) are represented as equations in terms of the compressive strength, the embedment length, the properties of FRP stiffness and adhesive as shown in Eq. (15) and Eq. (16), respectively.

$$G_{f-NSM} = 0.0785 \cdot (1/L_b)^{-0.874} (f_c')^{1.2483} \left(\frac{E_r A_r}{p_r}\right)^{-0.923} \left(\frac{G_a}{t_a}\right)^{0.071} \quad (15)$$

$$B_{NSM} = 226.29 \cdot (1/L_b)^{1.5287} \left(\frac{E_r A_r}{p_r}\right)^{0.6721} \left(\frac{G_a}{t_a}\right)^{-0.135} \quad (16)$$

The relations between various terms in Eq. (15) and Eq. (16) can be reasonably explained through the experimental results as following. The increase in the concrete compressive strength significantly affected the interfacial fracture energy due to the confinement of concrete. Similarly, the increase in the embedment length slightly enhanced the interfacial energy G_{f-NSM} . This observation was also found in the studies by Lorenzis et al. [1]. In contrast, the interfacial fracture energy of the bond behavior between NSM FRP-concrete increased when the stiffness of FRP decreased. This is because the strain development in FRP bars enhanced when the Young's modulus

of FRP was low. Meanwhile, the increase in the shear stiffness of adhesive did not have a significant influence on the interfacial energy for NSM FRP-concrete interface response.

On the other hand, the embedment length greatly affects the interfacial ductility of the NSM FRP-concrete bond behavior (B_{NSM}). Also, the stiffness of the NSM FRP bars has the same trend to the embedment length. The enhancement in the shear stiffness of adhesive displays the similar observation as in G_{f-NSM} formulation.

3.2 ETS strengthening method

3.2.1 Database

The previous studies of Bui et al. [7], Godat et al. [8], and Caro et al. [9], which examined the bond behavior of ETS FRP strengthening, are selected to propose the bond model. The database was chosen from the total results of 32 specimens including the parameters of the types of FRP bars, the concrete compressive strength ranging from 20.7 to 45.6 MPa, the bar diameter ranging from 8.0 to 12.7 mm, the embedment length ranging from 45 to 250 mm, the elastic modulus of FRP ranging from 40 to 155 GPa, the elastic modulus of adhesive ranging 2.18 to 3.10 GPa, and thickness of adhesive ranging 2.38 to 9.52 mm.

3.2.2 Proposed equations

The interfacial fracture energy for ETS bond behavior (G_{f-ETS}) is influenced by the concrete compressive strength, embedment length, the properties of FRP stiffness, and adhesive parameters, as shown in Bui et al. [7]. Following the regression procedure, Eq. (17) demonstrates the equation for the interfacial energy. It is apparent from Eq. (17) that the concrete compressive strength has the greatest effect on the interfacial fracture energy due to the confinement of concrete to ETS bars. Moreover, the embedment length also affects the fracture energy. The increase in embedment length induces the enhancement of the interfacial energy. Nevertheless, both the FRP stiffness and adhesive stiffness in ETS technique slightly impact the interfacial fracture energy.

$$G_{f-ETS} = 6\times10^{-5}\cdot\left(\frac{1}{L_b}\right)^{-1.059}\left(f_c^{'}\right)^{1.5339}\left(\frac{E_rA_r}{p_r}\right)^{0.1145}\left(\frac{G_a}{t_a}\right)^{0.0085} \quad (17)$$

On the other hand, the formulation for the interfacial bond ductility using the proposed regression analysis of ETS specimens is shown in Eq. (18). The most effective factor to B_{ETS} equation is the embedment length, in which the long embedment greatly increased the ETS interfacial ductility. Similar to the results exhibited in the study by Bui et al. [7], long embedment length was capable in the lag of strain development, resulting in the considerable ductility. Additionally, the stiffness of ETS FRP bars slightly affected the B_{ETS} . While, the stiffness of adhesive barely impacts the B_{ETS} with a contrast tendency to the influence of ETS stiffness.

$$B_{ETS} = 453.09\cdot\left(\frac{1}{L_b}\right)^{1.3308}\left(\frac{E_rA_r}{p_r}\right)^{0.3085}\left(\frac{G_a}{t_a}\right)^{-0.217} \quad (18)$$

In the following section, the formulations of G_f and B are adopted to generate the bond-slip model showing the interfacial performance of the strengthening methods, ETS and NSM.

4. Parametric study

This section presents the use of bond stress-slip relationship to describe the effects of various parameters to the efficiency of the NSM and ETS strengthening techniques. The investigating factors are FRP bar types, embedment length, and concrete compressive strength. The bond stress-slip relationship is defined by Eq. (6) along with using the formulations of G_f and B in the previous section.

4.1 NSM strengthening technique

Fig. 5(a) presents the effects of the FRP stiffness to the bond behavior of the NSM method. The large stiffness of NSM FRP resulted in the high rigidity of the bond stress-slip relationships. The increase in Young's modulus of FRP bars provided the decrease in the bond stress of the specimens. This is mainly because that the high stiffness of FRP offered the low strain in the FRP, making the bond stress to be low. This finding indicates that the GFRP bar, which has low modulus, can be suitable for embedding in concrete specimen using the NSM strengthening technique in terms of the bond performance and ductility.

On the other hand, the increase in embedment length for the NSM technique decreased the bond stress as shown in **Fig. 5(b)**. It is due to the great strain development with insufficient embedment length, resulting in the high bond stress. In addition, the bond ductility values decreased as the embedment length enhanced. This was also reported in the previous studies by Dai et al. [5] and Bui et al. [7].

Fig. 5(c) presents the bond stress-slip responses with different concrete compressive strengths. It is obvious from the

analytical investigation and the test results that the bond stress increased when enhancing the concrete compressive strength by pullout test. This may mainly be because the confinement action of the high strength concrete triggered the shear transfer mechanism of concrete-adhesive-NSM FRP.

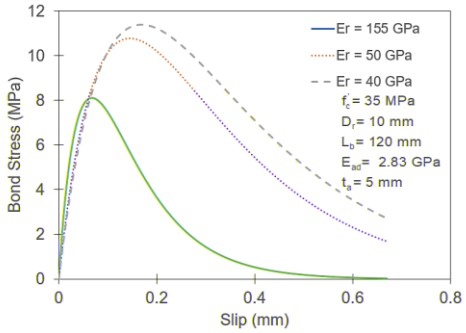

(a) FRP bar type

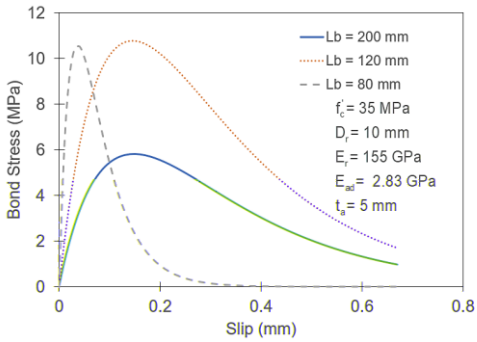

(b) Embedment length

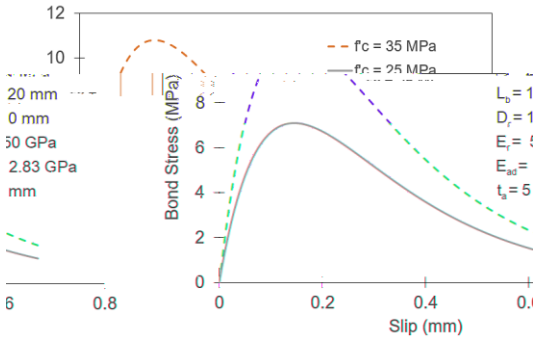

(c) Concrete compressive strength

Fig. 5 Effect of FRP bar type, embedment length and concrete compressive strength on bond stress-slip relationship of NSM

specimens were fully embedded into the concrete core, leading to the considerable confinement. This phenomenon exhibits the feasible shear transfer mechanism of concrete-adhesive-ETS FRP. **Fig. 6(a)** also implies that the ETS CFRP specimen induced the largest bond stress-slip efficiency.

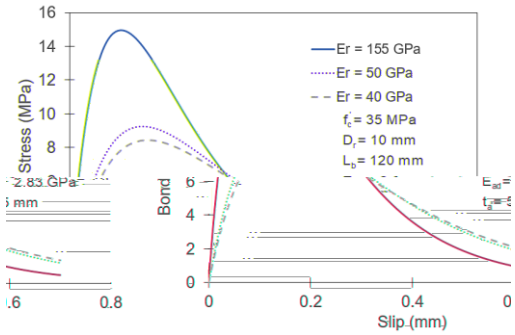

(a) FRP bar type

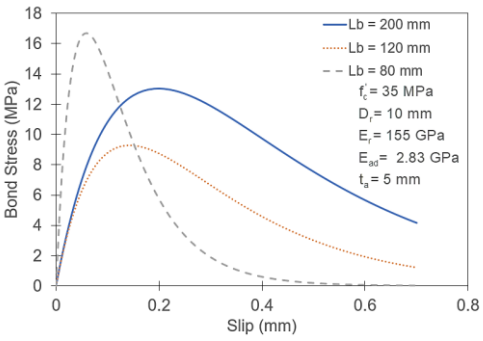

(b) Embedment length

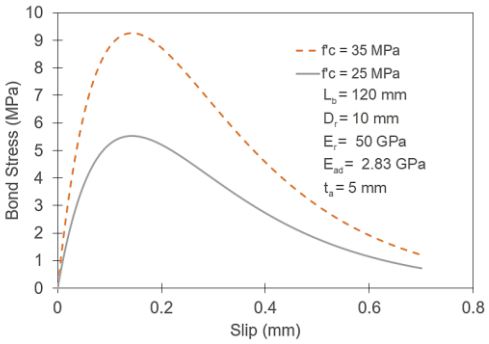

(c) Concrete compressive strength

Fig. 6 Effect of FRP bar type, embedded length and concrete compressive strength on bond stress-slip relationship of ETS

4.2 ETS strengthening technique

Fig. 6(a) shows the effects of bar stiffness on the bond behavior for the ETS technique**.** The increasing stiffness of FRP bar provides the increase of bond stress, which attributes to the inverse of NSM technique. It is because the FRP bars in the ETS

For the effect of the embedment length, it is similar to the NSM method that the increase in embedment length of the ETS bars decreased the bond stress as displayed in **Fig. 6(b)**. However, comparing to the NSM method, the reduction in bond stress with increasing embedment length for the ETS method is

not significant. It may be due to the proper confinement of the specimen to ETS FRP, redistributing the shear resisting transfer.

Additionally, the bond performance of the ETS technique was improved by enhancing the concrete compressive strength as shown in **Fig. 6(c)**. For this reason, the concrete specimens could be able to withstand the forces acting and completely fail by pullout and splitting.

4.3 Comparison between NSM and ETS techniques

Figs. 7(a) and 7(b) illustrate the bond stress-slip curves of the two strengthening techniques with the same parameters except the Young's modulus values of the FRP. It is apparent that when the modulus of elasticity of FRP bars for both strengthening techniques was approximately 155 GPa (high stiffness), the specimen embedded by the ETS FRP bar provided the higher bond stress than that of the NSM technique, approximately 54%. Whereas, when the Young's modulus for both techniques is roughly 50 GPa (low stiffness), the specimen inserted by NSM FRP bar offers the greater bond stress than that of the ETS technique, approximately 14%. It can be analytically implied that the embedment with CFRP bars is appropriate for the ETS techniques, while the embedment with GFRP bars is suitably notable for the NSM strengthening technique.

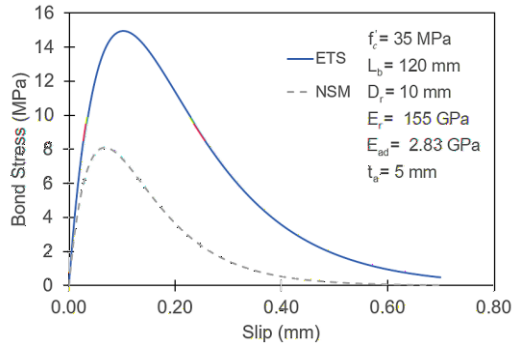

(a) E_r = 155 GPa

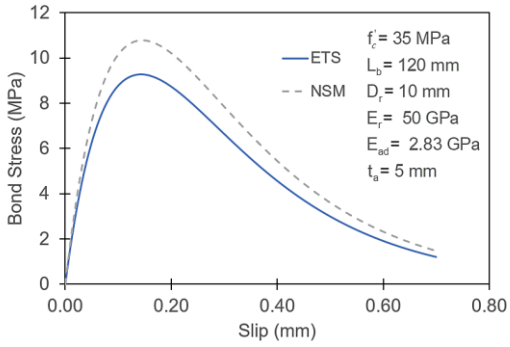

(b) E_r = 50 GPa

Fig. 7 Effects of bond stress–slip responses in each strengthening method

5. Conclusion

The bond models for the ETS and NSM strengthening methods are developed through an analytical investigation using the nonlinear regression procedure. Based on the results in this study, the following conclusions can be drawn.

(1) The formulations for two factors, interfacial ductility (B) and interfacial energy (G_f), considering various important parameters are proposed. Additionally, a parametric study utilizing the proposed equations to the bond model was carried out. The large stiffness of FRP resulted in the high rigidity of the bond stress-slip relationships for both techniques. However, the increasing stiffness of FRP bar furnished the increase of bond stress of ETS method, which was contrast to that for the NSM technique. The decrease in bond stress with increasing embedment length for the ETS method is not significant compared to that for the NSM method. The effect of the concrete compressive strength for two strengthening methods offered a consistent bond efficiency.

(2) Through analytical investigation, the embedment with CFRP bars is deemed to be appropriate for the ETS techniques, while the embedment with GFRP bars is seemly reasonable for the NSM strengthening technique.

References

[1] De Lorenzis, L., Rizzo, A. and La Tegola, A. (2002). A modified pull-out test for bond of near-surface mounted FRP rods in concrete. *Composites Part B: Engineering*, *33*(8), 589-603.

[2] Soliman, S. M., El-Salakawy, E. and Benmokrane, B. (2011). Bond performance of near-surface-mounted FRP bars. *Journal of Composites for Construction, 15*(1), 103-111.

[3] Hassan, T. and Rizkalla, S. (2004). Bond mechanism of NSM FRP bars for flexural strengthening of concrete structures. *ACI Structural Journal, 101*(6), 830-839.

[4] Kalupahana, W. K. G. (2009). *Anchorage and bond behaviour of near surface mounted fibre reinforced polymer bars.* (Doctoral dissertation, University of Bath).

[5] Dai, J., Ueda, T. and Sato, Y. (2005). Development of the nonlinear bond stress–slip model of fiber reinforced plastics sheet–concrete interfaces with a simple method. *Journal of composites for construction*, 9(1), 52-62.

[6] Dai, J. G., Sato, Y. and Ueda, T. (2002). Improving the load transfer and effective bond length for FRP composites bonded to concrete. *Proceedings of the Japan Concrete Institute, 24*(1), 1423-1428.

[7] Bui, L. V. H., Stitmannaithum, B. and Jongvivatsakul, P. (2020). Comprehensive investigation on bond mechanism of embedded through-section fiber-reinforced polymer bars to concrete for structural analysis. *Journal of Building Engineering*, 101180.

[8] Godat, A., L'hady, A., Chaallal, O. and Neale, K. W. (2012). Bond behavior of the ETS FRP bar shear-strengthening method. *Journal of Composites for Construction, 16*(5), 529-539.

[9] Caro, M., Jemaa, Y., Dirar, S. and Quinn, A. (2017). Bond performance of deep embedment FRP bars epoxy-bonded into concrete. *Engineering Structures, 147*, 448-457.